GEOLOGY | THE GEOLOGICAL SOCIETY OF AMERICA®

https://doi.org/10.1130/G48243.1

Manuscript received 6 August 2020
Revised manuscript received 14 October 2020
Manuscript accepted 21 October 2020

Published online 16 December 2020

Drill core from seismically active sandstone gas reservoir yields clues to internal deformation mechanisms

Berend A. Verberne[1,2], Suzanne J.T. Hangx[1]*, Ronald P.J. Pijnenburg[1], Maartje F. Hamers[1], Martyn R. Drury[1] and Christopher J. Spiers[1]

[1]Department of Earth Sciences, Utrecht University, P.O. Box 80.115, 3508 TC Utrecht, Netherlands

[2]Geological Survey of Japan, National Institute of Advanced Industrial Science and Technology, 1-1-1 Higashi, Tsukuba, Ibaraki 305-8567, Japan

ABSTRACT

Europe's largest gas field, the Groningen field (the Netherlands), is widely known for induced subsidence and seismicity caused by gas pressure depletion and associated compaction of the sandstone reservoir. Whether compaction is elastic or partly inelastic, as implied by recent experiments, is a key factor in forecasting system behavior and seismic hazard. We sought evidence for inelastic deformation through comparative microstructural analysis of unique drill core recovered from the seismogenic center of the field in 2015, 50 yr after gas production started, versus core recovered before production (1965). Quartz grain fracturing, crack healing, and stress-induced Dauphiné twinning are equally developed in the 2015 and 1965 cores, with the only measurable effect of gas production being enhanced microcracking of sparse K-feldspar grains in the 2015 core. Interpreting these grains as strain markers, we suggest that reservoir compaction involves elastic strain plus inelastic compression of weak clay films within grain contacts.

INTRODUCTION

Hydrocarbon production reduces reservoir fluid pressure and increases the *in situ* (effective) stress, frequently leading to surface subsidence and induced seismicity (Geertsma, 1973; Yerkes and Castle, 1976). Subsidence is caused by one-dimensional (1-D) vertical compaction of the reservoir rock, whereas seismicity reflects coupled stress buildup at preexisting faults (Segall, 1989; Zoback, 2007). Reservoir compaction is widely assumed to be poro-elastic and, hence, reversible (Segall, 1992; Zoback, 2007). However, experiments on sandstones show that irreversible deformation contributes continuously during loading in the assumed poro-elastic range of 0.1%–0.2% strain (Bernabé et al., 1994; Shalev et al., 2014; Hol et al., 2018; Pijnenburg et al., 2018, 2019a), with sharp "plastic" yield occurring only at strains >1%–2%; i.e., far beyond those relevant for production-induced compaction (<0.5%). Including constitutive relations describing small-strain inelastic deformation may substantially modify forecasts of production-induced stress evolution (Pijnenburg et al., 2019a), subsidence, and induced seismicity. However, direct observations of the mechanisms responsible for irreversible, production-induced deformation are lacking.

One of the world's best-known gas fields showing production-induced compaction, subsidence, and seismicity is the vast Groningen field, the Netherlands (Fig. 1A). The reservoir is the 100–350-m-thick Slochteren Sandstone (Gaupp and Okkerman, 2011), located at ~3 km depth, where the overburden pressure is ~65 MPa (Fig. 1B; Van Eijs, 2015). Conglomeratic and mudstone facies dominate the south and north of the field, whereas the most porous, central part is typified by fluvial and eolian sands (de Jager and Visser, 2017). Since gas production started in the 1960s, gas pressure has fallen from 35 to ~8 MPa, and subsidence, driven by the increase in vertical effective stress, has reached ~33 cm in the center of the field (Fig. 1A). This implies vertical reservoir compaction strains of 0.1%–0.3%, consistent with *in situ* fiber-optic strain measurements (Cannon and Kole, 2017). Since ca. 1990, production has been accompanied by seismic events within the reservoir (Spetzler and Dost, 2017), causing property damage and public concern, notably in 2012, when the largest-magnitude earthquake (local magnitude M_L 3.6) occurred near Huizinge village. In 2015, field operator Nederlandse Aardolie Maatschappij BV (NAM) launched an unprecedented drilling operation at the Zeerijp ZRP-3a well (Figs. 1A and 1B) to retrieve reservoir core from the highly depleted, most seismogenic, central part of the field.

We report an investigation of Slochteren Sandstone samples from the ZRP-3a well, aimed at searching for evidence of small-strain (0.1%–0.3%), inelastic deformation processes. We used Slochteren Sandstone core recovered before depletion (1965), from the nearby Stedum SDM-1 well, as an undeformed benchmark. Potential mechanisms of inelastic reservoir compaction include (1) fracture of grains forming the load-supporting rock framework, (2) grain-scale dissolution-precipitation, and (3) processes operating within grain contacts, like asperity crushing/dissolution, clay film deformation, and slip (Spiers et al., 2017). We tested which of these may have operated by investigating the microstructure of reservoir core recovered from multiple depths in both wells (Fig. S1 in the Supplemental Material[1]), thus deliberately sampling the lithological variations that characterize the central part of the field.

METHODS AND RESULTS

We studied sandstones samples from the SDM-1 and ZRP-3a cores using techniques ranging from visual inspection to optical and backscattered electron (BSE) microscopy, X-ray mapping, cathodoluminescence (CL) imaging,

*E-mail: s.j.t.hangx@uu.nl

[1]Supplemental Material. Detailed description of the materials and methods employed in this study, Figures S1–S8, and Tables S1–S4. Please visit https://doi.org/10.1130/GEOL.S.13262861 to access the supplemental material, and contact editing@geosociety.org with any questions.

CITATION: Verberne, B.A., et al., 2021, Drill core from seismically active sandstone gas reservoir yields clues to internal deformation mechanisms: Geology, v. 49, p. 483–487, https://doi.org/10.1130/G48243.1

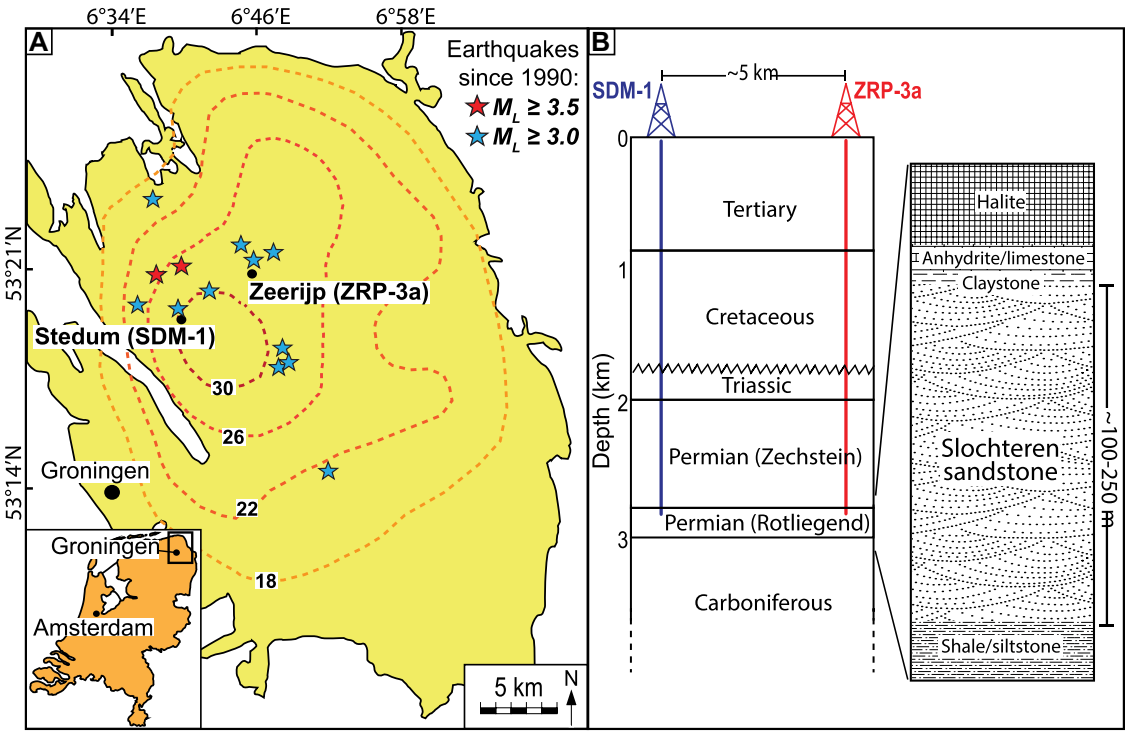

Figure 1. Groningen gas field in the Netherlands. (A) Subsidence contours in centimeters until 2013, and local magnitude $M_L \geq 3.0$ earthquake epicenters (stars) since 1990 (https://nam-feitenencijfers.data-app.nl/geotool/nam.html). (B) Stratigraphy showing the Slochteren Sandstone reservoir.

electron backscatter diffraction (EBSD) mapping, and image analysis.

Qualitative Analysis

Depleted and undepleted sandstone samples were indistinguishable at hand-specimen scale. A single SDM-1 core plug, laboratory-deformed to ~0.2% elastic plus ~0.2% inelastic strain, under conditions simulating depletion at well ZRP-3a, was also visually indistinguishable from its SDM-1 precursor (section S1 in the Supplemental Material; Fig. S2). To investigate grain-scale microstructures, 28 polished sections were prepared for optical and BSE imaging, using core fragments taken from 13 near-evenly distributed depth intervals (15–20 m) in each well, and using the laboratory-deformed sample and its undeformed counterpart for comparison (Fig. S1; Tables S1 and S2). All samples showed millimeter- to centimeter-scale sedimentary layering, enabling the effects of varying porosity, grain size/shape, and mineralogy on deformation signatures to be investigated. All were dominated by rounded to subangular quartz grains (≥70%), with minor quantities of K-feldspar (KFs; ≤15%), Ca-Mg-Fe carbonates (3–6%), lithic fragments (3–10%), and clay (illite, kaolinite; 0.5–5.5%; Fig. 2; Fig. S3), with a clastic grain size of 100–200 µm (Fig. 2; Tables S1 and S2). Carbonates were mainly present as authigenic cement in specific sedimentary layers. The scattered feldspar and lithic grains were frequently "corroded" and porous. Clay platelets were widespread, forming vermicules in pores and thin layers coating grains and grain contacts (average thickness 2–5 µm;

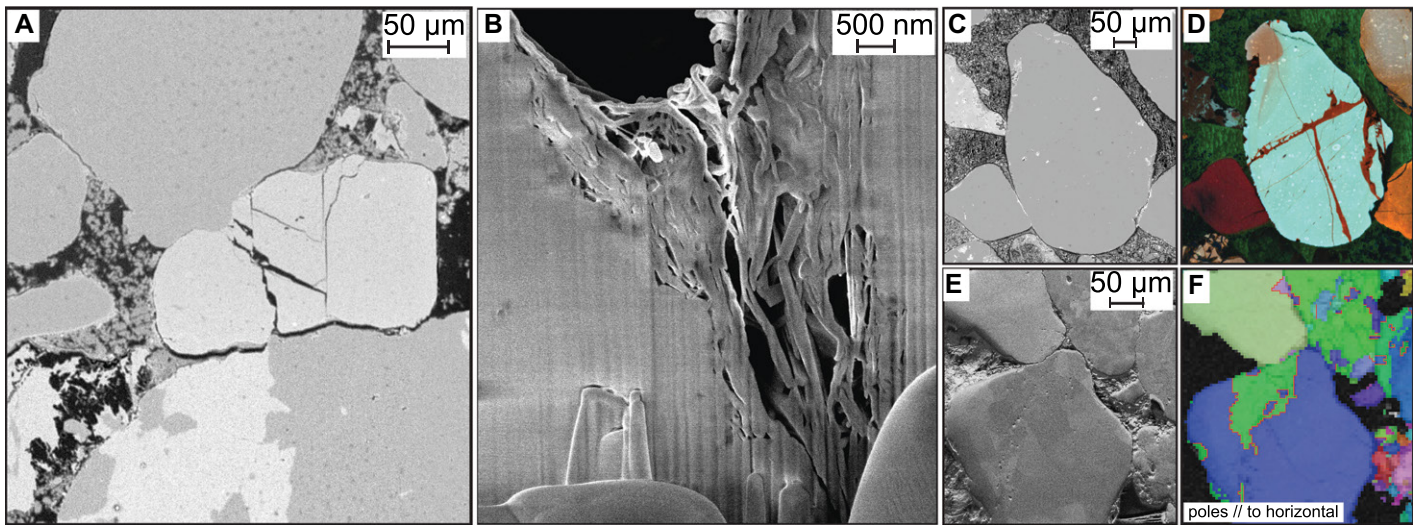

Figure 2. Slochteren Sandstone (Groningen gas field, the Netherlands) microstructure. (A) Cracks in K-feldspar (sample I, backscattered electron [BSE] image). (B) Sectioned quartz-quartz grain contact revealing clay film (sample Sw01, secondary electron image). (C) BSE and (D) cathodoluminescence intensity map (red high, blue low) showing multiple generations of quartz precipitation and (refractured) healed cracks (sample Z22). (E) Forescattered electron image and (F) band-contrast map with inverse pole figure map and Dauphiné twin boundary overlay in red (sample Sw14A).

Waldmann and Gaupp, 2016). Intergranular films mainly consisted of preburial, tangential clay, with postburial, radial clay present on pore walls. Indented and sutured grain contacts indicating diagenetic pressure solution were widespread. Intergranular and transgranular cracks were rarely observed, but intragranular cracks were widespread, regardless of mineral type, depth interval, or source well. Both fresh and reacted feldspars frequently showed multiple intragranular cleavage cracks, made visible by dissolution. From qualitative inspection of optical or BSE micrographs, no distinction could be made between the depleted, undepleted, or laboratory-deformed samples.

Quantitative Microstructural Analysis

To assess the role of grain fracturing during reservoir depletion, porosity (ϕ), grain-size distribution (GSD), and intragranular crack density (crack count per unit grain area, ρ_{cr}) were quantified within microstructurally distinctive sedimentary domains measuring ~10–190 mm^2, as observed in section-scale BSE mosaics (section S2; Fig. S4; Tables S1 and S2). We identified tens of thousands of intragranular cracks within ~50 domains in each of the SDM-1 and ZRP-3a core samples, plus seven in the laboratory-deformed sample. No correlations were found between ρ_{cr} and mean/median grain size, or with the standard deviation, skewness, or kurtosis of the GSD, in any of the materials studied (Fig. S5). Crack densities ranged from ~1 to 30 mm^{-2} for porosities of 4–29%, with the ρ_{cr}-ϕ data for the entire suite of samples studied falling in a band (Fig. 3A), suggesting a tendency for crack density to increase with increasing porosity. However, the data for the depleted, undepleted, and laboratory-deformed samples were indistinguishable (Fig. 3A, inset). This suggests that grain failure did not play a significant role in producing inelastic strain in the ZRP-3a core versus the undepleted SDM-1 core, or in the laboratory test on SDM-1 material.

Crack density analysis combined with electron dispersive X-ray mapping revealed that KFs grains frequently showed multiple intragranular (cleavage) fractures (Figs. 2A and 3B; Fig. S3). To avoid bias due to varying KFs grain area (A_{grain}^{KFs}) per sample, for each domain we determined the fraction of cracks cutting KFs grains ($\mu_1 = N_{cr}^{KFs}/N_{cr}^{tot}$) versus the KFs area fraction ($\mu_2 = A_{grain}^{KFs}/A_{grain}^{tot}$) (Fig. 3C). For both the depleted and undepleted samples, we found $\mu_1 > \mu_2$, implying that KFs grains were preferentially cracked compared with quartz and other minerals. Moreover, two-sample hypothesis testing of the ZRP-3a versus SDM-1 sample population means showed statistical discernibility at a 94% confidence level (section S4). This suggests that KFs grains in samples from the depleted core are preferentially cracked compared with samples from the undepleted core (Fig. 3C). Coupled with local intergranular displacements, this could "nucleate" bulk inelastic deformation. However, in view of the low abundance of KFs compared with quartz (~15%), and their spatially scattered distribution in the reservoir rock, this is unlikely. More likely, feldspar grains act as passive markers indicative of deformation of the surrounding grain framework. With the grain strength of quartz being higher than feldspar (Hangx et al., 2010), especially when the latter is corroded by reaction, even small, elastic strains within the surrounding quartz-grain framework should lead to fracturing of the feldspar grains.

The possibility that enhanced stresses at quartz grain contacts due to gas depletion caused reactivation of healed intragranular cracks, or of pressure-dissolved contacts, was also investigated. Using high-resolution panchromatic CL imaging, we scrutinized ZRP-3a and SDM-1 samples for quartz overgrowths and (reactivated) healed fractures (Figs. 2C and 2D; Figs. S6 and S7). We found no evidence for more, or more recent, diffusive mass transport in depleted (ZRP-3a) versus undepleted (SDM-1) samples, nor for statistically significant differences in the reactivation of healed fractures (Table S3). In quartz, high compressive stresses can trigger Dauphiné twinning (Tullis, 1970), offering a potential indicator of enhanced grain-contact stresses (Mørk and Moen, 2007). EBSD mapping of Dauphiné twin (DT) boundaries showed that DTs were present in all samples analyzed, at grain contacts and within grain interiors (Figs. 2E and 2F; Fig. S8). The DT density (ρ_{DT}), defined as the ratio of the total DT boundary length to the total quartz grain area, measured 10.6 mm^{-1} in depleted core, 9.44 and 16.8 mm^{-1} in undepleted core, and 14.5 mm^{-1} in the laboratory-deformed sample (Table S4). We infer that (simulated) depletion was insufficient to measurably enhance Dauphiné twinning.

DISCUSSION AND CONCLUSIONS

Our results imply that neither fracturing nor dissolution of the quartz framework grains played a significant role in causing production-induced compaction at the center of the Groningen field. The only measurable microstructural difference between samples from the undepleted SDM-1 and depleted ZRP-3a wells is the breakage of KFs. We suggest that preferred fracturing of these scattered, corroded, cleavage-prone, and hence weaker, KFs grains occurred as a result of the vertical poro-elastic compaction of the quartz-grain framework that occurred during reservoir depletion. Our interpretation is that the preferentially fractured KFs grains persisted as a qualitative record of the elastic strain accommodated by the rock framework,

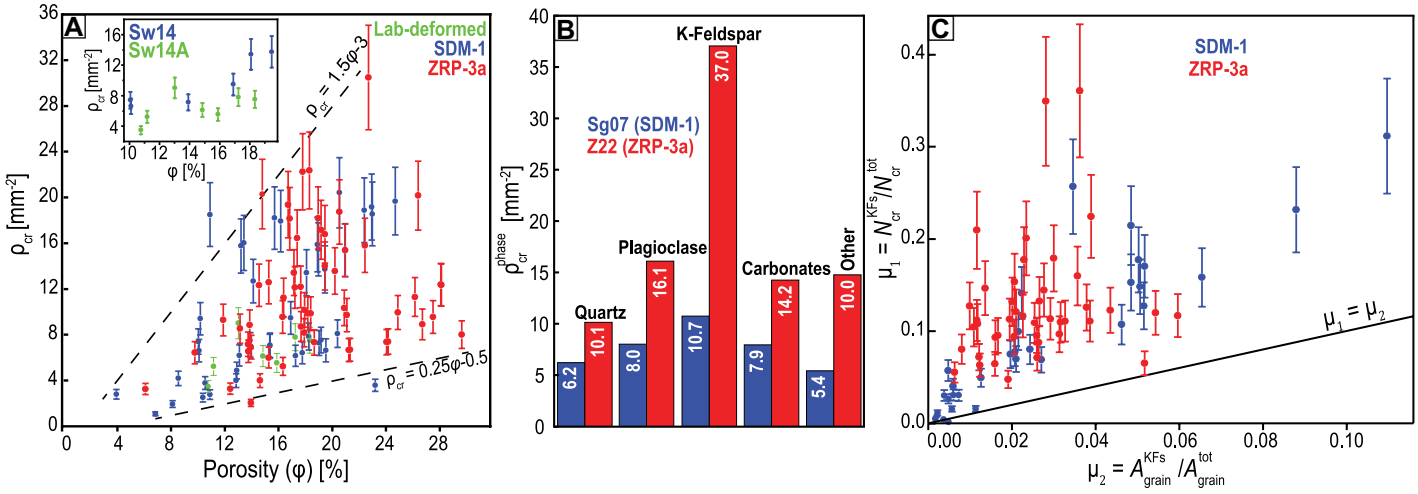

Figure 3. Intragranular crack density (ρ_{cr}). (A) ρ_{cr} data measured in distinct sedimentary domains identified in sectioned SDM-1 and ZRP-3a well samples from the Groningen gas field, the Netherlands, and in laboratory-deformed SDM-1 sample (section Sw14a). (B) Phase-specific crack density (ρ_{cr}^{phase}) in sections Sg07 (SDM-1) and Z22 (ZRP-3a). (C) Fraction of cracks in K-feldspar (μ_1) versus the K-feldspar (KFs) area fraction (μ_2).

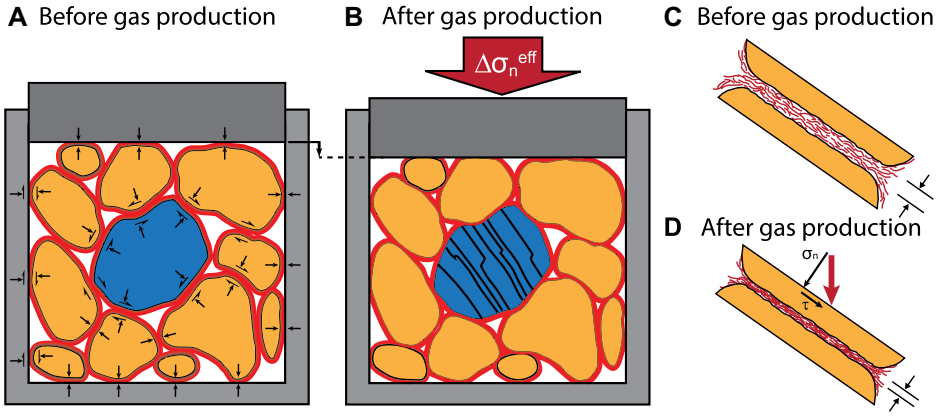

Figure 4. Schematic diagram illustrating inferred reservoir compaction mechanism. Note, in this simplification, all grain surfaces are coated with uniform clay films. In a real sandstone reservoir, clay films are discontinuous and locally absent, especially in distal regions of the field. (A,B) Idealized volume of reservoir sandstone undergoing uniaxial compaction strain path typical of producing gas reservoirs (vertical compaction with zero horizontal strain). Orange—load-supporting quartz framework; blue—sparse feldspar grains; red—clay films. Normal and shear displacements are indicated at selected grain contacts. (C,D) Deformation at grain-contact scale. Increase in vertical effective stress ($\Delta\sigma_n^{eff}$) due to pore-pressure depletion leads to uniaxial compaction of bulk rock (A→B), accommodated by elastic deformation of quartz grain framework plus compaction and shear of clay films trapped in load-bearing grain contacts (C→D). Increased stresses driving clay film deformation lead to fracture of weaker, corroded K-feldspar grains (B), while stronger quartz grains remain intact. Shear within clay-filled grain contacts leads to increased lateral stresses due to zero lateral strain.

without significantly contributing to permanent deformation. At the same time, it is important to consider the effects of the weak clay films that coat most detrital grain contacts (Fig. 2; Fig. S3). Because the Groningen reservoir lies close to its maximum burial depth (Gaupp and Okkerman, 2011), and because long-term clay consolidation depends mainly on effective normal stress (Brown et al., 2017), intergranular clay films compacted during burial would almost certainly deform further as the effective vertical stress increased from ~30 to 57 MPa during depletion of the Groningen reservoir. As demonstrated by Pijnenburg et al. (2019b), such stress changes are sufficient to inelastically compact individual 2–5-µm-thick intergranular clay films in the Slochteren sandstone by ~4%, i.e., by 0.1–0.2 µm. Coupled with the intergranular sliding (clay film shearing) required by the *in situ* condition of 1-D vertical strain, this implies reservoir compaction strains of 0.1–0.2% for typical detrital grain sizes of 100–200 µm (Pijnenburg et al., 2019b). While these compaction strains match field subsidence and *in situ* strain data well, they are virtually impossible to detect in the postmortem microstructure, as there are no internal strain markers either at the grain or clay film scales.

Combining (1) the irreversible deformation observed in small-strain experiments simulating depletion (Hol et al., 2018; Pijnenburg et al., 2018, 2019a) and attributed to clay film deformation (Pijnenburg et al., 2019b), (2) the widespread occurrence of intergranular clay coatings in the Groningen reservoir (Waldmann and Gaupp, 2016), and (3) the burial history of the reservoir (Gaupp and Okkerman, 2011), we infer that elastic deformation of the Slochteren Sandstone plus inelastic deformation by intergranular clay film compression and shear offer the most viable explanation for the strains recorded by cracked feldspars in the depleted core (Fig. 4).

To date, studies addressing inelastic compaction of porous rock have focused on the microphysical mechanisms controlling macroscopic plastic yield at strains far in excess (>1–2%) of the strains occurring in hydrocarbon reservoirs (Brantut et al., 2013; Menéndez et al., 1996; Wong and Baud, 2012). These studies frequently show strain localization accommodated by grain fracturing and associated grain-scale rearrangement. For the case of small-strain, production-induced, seismogenic compaction of the Groningen and similar reservoirs, our study suggests that deformation at grain contacts, involving micrometer-scale clay film compaction and shear, may be a key factor (Fig. 4). The compressive strength of a wide range of reservoir sandstones was recently shown to decrease with increasing clay content (Heap et al., 2019), supporting the proposed mechanism. Physics-based models aiming to forecast induced subsidence and seismicity (Bourne et al., 2014; Zbinden et al., 2017; Buijze et al., 2019), as in the case of the Groningen field, should aim to incorporate constitutive models describing inelastic processes, such as the intergranular clay film deformation inferred here, because the impact on horizontal stress evolution is substantial (Pijnenburg et al., 2019a, 2019b).

ACKNOWLEDGMENTS

We thank J. van Elk, D. Doornhof, C. Visser, D. Doran, F. Marcellis, T. Wolterbeek, R. Keijzer, E. Gutiérrez, S. Matveev, S. Waldmann, and L. Bik. D. Healy, R. Gaupp, and an anonymous reviewer provided helpful comments. The work was funded by Groningen field operator Nederlandse Aardolie Maatschappij BV (NAM) (agreement UI49358). European Research Council starting grant SEISMIC 335915 supported Hamers.

REFERENCES CITED

Bernabé, Y., Fryer, D.T., and Shively, R.M., 1994, Experimental observations of the elastic and inelastic behaviour of porous sandstones: Geophysical Journal International, v. 117, p. 403–418, https://doi.org/10.1111/j.1365-246X.1994.tb03940.x.

Bourne, S.J., Oates, S.J., van Elk, J., and Doornhof, D., 2014, A seismological model for earthquakes induced by fluid extraction from a subsurface reservoir: Journal of Geophysical Research: Solid Earth, v. 119, p. 8991–9015, https://doi.org/10.1002/2014JB011663.

Brantut, N., Heap, M.J., Meredith, P.G., and Baud, P., 2013, Time-dependent cracking and brittle creep in crustal rocks: A review: Journal of Structural Geology, v. 52, p. 17–43, https://doi.org/10.1016/j.jsg.2013.03.007.

Brown, K.M., Poeppe, D., Josh, M., Sample, J., Even, E., Saffer, D., Tobin, H., Hirose, T., Kulongoski, J.T., Toczko, S., and Maeda, L., 2017, The action of water films at Å-scales in the Earth: Implications for the Nankai subduction system: Earth and Planetary Science Letters, v. 463, p. 266–276, https://doi.org/10.1016/j.epsl.2016.12.042.

Buijze, L., van den Bogert, P.A.J., Wassing, B.B.T., and Orlic, B., 2019, Nucleation and arrest of dynamic rupture induced by reservoir depletion: Journal of Geophysical Research: Solid Earth, v. 124, p. 3620–3645, https://doi.org/10.1029/2018JB016941.

Cannon, M., and Kole, P., 2017, The First Year of Distributed Strain Sensing (DSS) Monitoring in the Groningen Gas Field: Houston, Texas, Shell International Exploration and Production, Inc., 73 p.

de Jager, J., and Visser, C., 2017, Geology of the Groningen field—An overview: Netherlands Journal of Geosciences, v. 96, p. s3–s15, https://doi.org/10.1017/njg.2017.22.

Gaupp, R., and Okkerman, J.A., 2011, Diagenesis and reservoir quality of Rotliegend sandstones in the northern Netherlands—A review, *in* Grötsch, J., and Gaupp, R., eds., The Permian Rotliegend of the Netherlands: Society for Sedimentary Geology (SEPM) Special Publication 98, p. 193–226, https://doi.org/10.2110/pec.11.98.0193.

Geertsma, J., 1973, Land subsidence above compacting oil and gas reservoirs: Journal of Petroleum Technology, v. 25, p. 734–744, https://doi.org/10.2118/3730-PA.

Hangx, S.J.T., Spiers, C.J., and Peach, C.J., 2010, Creep of simulated reservoir sands and coupled chemical-mechanical effects of CO_2 injection: Journal of Geophysical Research: Solid Earth, v. 115, B09205, https://doi.org/10.1029/2009JB006939.

Heap, M.J., Villeneuve, M., Kushnir, A.R.L., Farquharson, J.I., Baud, P., and Reuschlé, T., 2019, Rock mass strength and elastic modulus of the Buntsandstein: An important lithostratigraphic unit for geothermal exploitation in the Upper Rhine Graben: Geothermics, v. 77, p. 236–256, https://doi.org/10.1016/j.geothermics.2018.10.003.

Hol, S., van der Linden, A., Bierman, S., Marcelis, F., and Makurat, A., 2018, Rock physical controls on production-induced compaction in the Groningen

Field: Scientific Reports, v. 8, p. 7156, https://doi.org/10.1038/s41598-018-25455-z.
Menéndez, B., Zhu, W., and Wong, T.-F., 1996, Micromechanics of brittle faulting and cataclastic flow in Berea sandstone: Journal of Structural Geology, v. 18, p. 1–16, https://doi.org/10.1016/0191-8141(95)00076-P.
Mørk, M.B.E., and Moen, K., 2007, Compaction microstructures in quartz grains and quartz cement in deeply buried reservoir sandstones using combined petrography and EBSD analysis: Journal of Structural Geology, v. 29, p. 1843–1854, https://doi.org/10.1016/j.jsg.2007.08.004.
Pijnenburg, R.P.J., Verberne, B.A., Hangx, S.J.T., and Spiers, C.J., 2018, Deformation behavior of sandstones from the seismogenic Groningen gas field: Role of inelastic versus elastic mechanisms: Journal of Geophysical Research: Solid Earth, v. 123, p. 5532–5558, https://doi.org/10.1029/2018JB015673.
Pijnenburg, R.P.J., Verberne, B.A., Hangx, S.J.T., and Spiers, C.J., 2019a, Inelastic deformation of the Slochteren Sandstone: Stress-strain relations and implications for induced seismicity in the Groningen gas field: Journal of Geophysical Research: Solid Earth, v. 124, p. 5254–5282, https://doi.org/10.1029/2019JB017366.
Pijnenburg, R.P.J., Verberne, B.A., Hangx, S.J.T., and Spiers, C.J., 2019b, Intergranular clay films control inelastic deformation in the Groningen gas reservoir: Evidence from split-cylinder deformation tests: Journal of Geophysical Research: Solid Earth, v. 124, p. 12679–12702, https://doi.org/10.1029/2019JB018702.
Segall, P., 1989, Earthquakes triggered by fluid extraction: Geology, v. 17, p. 942–946, https://doi.org/10.1130/0091-7613(1989)017<0942:ETBFE>2.3.CO;2.
Segall, P., 1992, Induced stresses due to fluid extraction from axisymmetric reservoirs: Pure and Applied Geophysics, v. 139, p. 535–560, https://doi.org/10.1007/BF00879950.
Shalev, E., Lyakhovsky, V., Ougier-Simonin, A., Hamiel, Y., and Zhu, W., 2014, Inelastic compaction, dilation and hysteresis of sandstones under hydrostatic conditions: Geophysical Journal International, v. 197, p. 920–925, https://doi.org/10.1093/gji/ggu052.
Spetzler, J., and Dost, B., 2017, Hypocentre estimation of induced earthquakes in Groningen: Geophysical Journal International, v. 209, p. 453–465, https://doi.org/10.1093/gji/ggx020.
Spiers, C.J., Hangx, S.J.T., and Niemeijer, A.R., 2017, New approaches in experimental research on rock and fault behaviour in the Groningen gas field: Netherlands Journal of Geosciences, v. 96, p. s55–s69, https://doi.org/10.1017/njg.2017.32.
Tullis, J., 1970, Quartz: Preferred orientation in rocks produced by Dauphiné twinning: Science, v. 168, p. 1342–1344, https://doi.org/10.1126/science.168.3937.1342.
Van Eijs, R., 2015, Neotectonic Stresses in the Permian Slochteren Formation of the Groningen Field: NAM, Koninklijk Nederlands Meteorologisch Instituut Scientific Report EP201510210531, 33 p.
Waldmann, S., and Gaupp, R., 2016, Grain-rimming kaolinite in Permian Rotliegend reservoir rocks: Sedimentary Geology, v. 335, p. 17–33, https://doi.org/10.1016/j.sedgeo.2016.01.016.
Wong, T.-f., and Baud, P., 2012, The brittle-ductile transition in porous rock: A review: Journal of Structural Geology, v. 44, p. 25–53, https://doi.org/10.1016/j.jsg.2012.07.010.
Yerkes, R.F., and Castle, R.O., 1976, Seismicity and faulting attributable to fluid extraction: Engineering Geology, v. 10, p. 151–167, https://doi.org/10.1016/0013-7952(76)90017-X.
Zbinden, D., Rinaldi, A.P., Urpi, L., and Wiemer, S., 2017, On the physics-based processes behind production-induced seismicity in natural gas fields: Journal of Geophysical Research: Solid Earth, v. 122, p. 3792–3812, https://doi.org/10.1002/2017JB014003.
Zoback, M.D., 2007, Reservoir Geomechanics: Cambridge, UK, Cambridge University Press, 449 p., https://doi.org/10.1017/CBO9780511586477.

Printed in USA